

.....

First underground results with NEWAGE-0.3a direction-sensitive dark matter detector

Kentaro Miuchi^a, Hironobu Nishimura^a, Kaori Hattori^a, Naoki Higashi^a,
Chihiro Ida^a, Satoshi Iwaki^a, Shigeto Kabuki^a, Hidetoshi Kubo^a,
Shunsuke Kurosawa^a, Kiseki Nakamura^a, Joseph Parker^a, Tatsuya Sawano^a,
Michiaki Takahashi^a, Toru Tanimori^a, Kojiro Taniue^a, Kazuki Ueno^a,
Hiroyuki Sekiya^b, Atsushi Takeda^b, Ken'ichi Tsuchiya^c, Atsushi Takada^d

^a *Cosmic-Ray Group, Department of Physics, Graduate School of Science, Kyoto
University Kitashirakawa-oiwakecho, Sakyo-ku, Kyoto, 606-8502, Japan*

^b *Kamioka Observatory, ICRR, The University of Tokyo Higashi-Mozumi, Kamioka cho,
Hida 506-1205 Japan*

^c *National Research Institute of Police Science 6-3-1 Kashiwanoha, Kashiwa, Chiba,
277-0882, Japan*

^d *Scientific Balloon Laboratory, ISAS, JAXA Yoshinodai 3-1-1, Sagami-hara, Kanagawa,
229-8510, Japan*

Abstract

A direction-sensitive dark matter search experiment at Kamioka underground laboratory with the NEWAGE-0.3a detector was performed. The NEWAGE-0.3a detector is a gaseous micro-time-projection chamber filled with CF₄ gas at 152 Torr. The fiducial volume and target mass are $20 \times 25 \times 31$ cm³ and 0.0115 kg, respectively. With an exposure of 0.524 kg-days, improved spin-dependent weakly interacting massive particle (WIMP)-proton cross section limits by a direction-sensitive method were achieved including a new record of 5400 pb for 150 GeV/c² WIMPs. We studied the remaining background and found that ambient γ -rays contributed about one-fifth of the remaining background and radioactive contaminants inside the gas chamber contributed the rest.

Key words: time projection chamber, micro pattern detector, dark matter, WIMP, direction-sensitive

PACS: , 14.80.Ly 29.40.Cs, 29.40.Gx, 95.35.+d

Email address: miuchi@cr.scphys.kyoto-u.ac.jp (Kentaro Miuchi^a)

1. Introduction

The interest in the search for dark matter has been growing continuously since the late 1980s. Attention to this problem recently increased after the Wilkinson Microwave Anisotropy Probe all-sky observation [1], Sloan Digital Sky Survey large-scale structure measurements [2, 3], and supernovae data from two other experiments (Supernova Cosmology Project [4] and High-Z Supernovae Search [5]) together produced more precise cosmological parameter determinations. Weakly interacting massive particles (WIMPs) are one of the strongest candidates for dark matter. WIMPs are searched for mainly in three ways: collider experiments [6], indirect (astrophysical) experiments [7, 8], and direct searches in the laboratory. The Large Hadron Collider (LHC) experiment is expected to discover or set a stringent limit on the properties of super-symmetric particles, which are a good candidate for WIMPs. Indirect experiments might detect some clues to the nature of WIMPs. While these experiments would provide information about the masses and cross sections, we still need direct searches to demonstrate that these particles are the dark matter in the Universe.

Many direct search experiments for WIMPs have been concluded [9, 10, 11, 12], are currently being performed [13, 14, 15, 16], or are being planned. The experiments with liquid noble-gas detectors [10] and cryogenic detectors [13] will be scaled up to more than one kilogram to explore the region predicted by Minimal Supersymmetric extension of the Standard Model (MSSM) theory [17] in the next decade. These massive detectors only measure the energy transferred to the nucleus through WIMP-nucleus scattering, thus the most distinct signal of WIMPs is annual modulation of the energy spectrum. Because the amplitude of the annual modulation signals is very small (a few percent of the total event of WIMP-nucleus scattering), the result of an 11-cycles' annual modulation observation reported by the DAMA/LIBRA group [9, 14] is the only positive signature ever reported. Although other groups have tried to confirm the

DAMA/LIBRA results with various types of detectors, no group has observed an annual modulation signal yet. Many groups are preparing larger-mass detectors for a nuclear-model-independent study of dark matter. Furthermore, detection methods other than the annual modulation signature are also necessary for an astrophysical-model-independent study.

Another distinct signature of WIMPs is thought to result from the relative motion of the solar system with respect to the galactic halo. If we assume isotropic WIMP motion, the peak WIMP flux should come from the direction of solar motion, which happens to point toward the constellation Cygnus. The recoil rate would then peak in the opposite direction, and this distribution would be a distinct signal. Several experimental and theoretical works on the possibility of detecting this anisotropy, or the WIMP-wind, have been performed so far [18, 19, 20, 21, 22, 23, 24, 25]. Among these proposed methods, a gaseous detector is one of the most appropriate devices for detecting this WIMP-wind because nuclear recoil tracks can in principle be detected with better angular resolutions than by other detectors [26, 27, 28]. The DRIFT group has pioneered studies of gaseous detectors for WIMP-wind detection for more than ten years with multi-wire proportional chambers [29, 30]. We proposed a new project, NEw generation WIMP-search with Advanced Gaseous tracking device Experiment (NEWAGE) [23], which has advantages over the DRIFT detectors in the pitch of the detection sensors and a three-dimensional tracking scheme. After the construction of a prototype detector and the first dark matter search experiment in a surface laboratory, we installed our prototype detector in an underground laboratory and studied its performance precisely [31, 32]. In this paper, we report the results of our first underground direction-sensitive dark matter search experiment.

2. Detector

For this experiment we used the NEWAGE-0.3a detector, the first prototype of our $(0.3\text{m})^3$ -class gaseous time-projection-chamber(TPC) series. The detec-

tor system and performance studies are described in our previous work [32], so we briefly summarize the essential properties closely related to this dark matter search experiment in this section.

2.1. System

A schematic view of the NEWAGE-0.3a detector is shown in FIG. 1. The NEWAGE-0.3a detector is a gaseous three-dimensional tracking detector read by a $30.7 \times 30.7 \text{ cm}^2$ μ -PIC (TOSHIBA/DNP, SN060222-3). A μ -PIC is a two-dimensional imaging device which has orthogonally-formed readout strips with a pitch of $400 \text{ }\mu\text{m}$ [33]. Field-shaping patterns on fluoroplastic circuit boards form a detection volume above a gas electron multiplier (GEM) [34]. We used a GEM with an amplification area of $23 \times 28 \text{ cm}^2$ (Scienergy Co. Ltd.) as an intermediate amplifier. A fiducial volume of $20 \times 25 \times 31 \text{ cm}^3$ was defined in a detection volume of $23 \times 28 \times 31 \text{ cm}^3$. Among many potential candidates for the chamber gas, we used CF_4 , which has advantages for spin-dependent (SD) WIMP detection. CF_4 is also known to be a good TPC gas because of its small diffusion coefficient, which is an indispensable property for a good angular resolution detector. We filled a stainless steel vessel with CF_4 gas at 152 Torr. The target mass in the effective volume was 0.0115kg. A SORB-AC cartridge pump (SAES Getter MK5) was attached to the vessel to absorb the out-going gas from the detector components. Typical operation parameters, optimized to realize a stable operation with a combined gas gain of 2400 (μ -PIC \times GEM = 300×8), are shown in Fig. 1.

2.2. Performance

We studied the detector performance in the underground laboratory. The measurements were carried out in the same manner as the dark matter runs in terms of the triggering and data acquisition systems. One set of event data consists of track shape information (digital hit points) and energy information (summed analog waveform). We calibrated the energy using the α particles generated in a $^{10}\text{B}(\text{n},\alpha)^7\text{Li}$ reaction ($Q = 2.310$ or 2.792 MeV). We set a glass

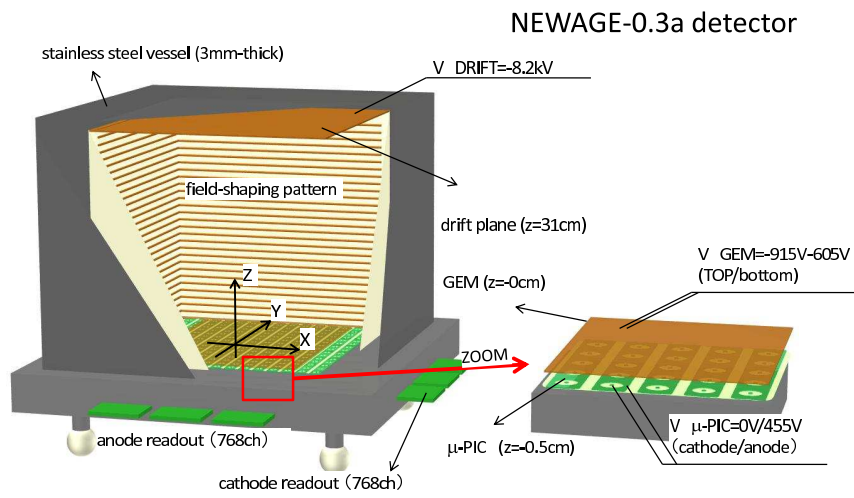


Figure 1: Schematic view of NEWAGE-0.3a detector. The volume between the drift plane and the GEM is the detection volume, it is filled with CF_4 gas at 152 Torr.

plate coated with a thin $0.6\text{ }\mu\text{m}$ ^{10}B layer in the gas volume, and irradiated the detector with thermalized neutrons. Alpha particles (5.6, 6.1, and 7.2 MeV) from decays of the radon progeny were also used. We thus used alpha-particle equivalent as the energy unit ($\text{keV}\alpha.\text{e}$) in this experiment. (We took account of the ionization efficiency, or quenching factor, of fluorine and helium nuclei in the analysis to calculate the expected spectra for WIMPs. We confirmed the linearity down in the dark matter energy range by the correlation of the track length and its energy.

We applied the following four event-selection criteria to the data. These criteria are the same as those applied to data from dark matter runs.

- N_{hit} selection: We selected events that have at least three hit points. We needed this criterion to determine the track directions with a certain angular resolution.
- Fiducial-volume selection: We selected events whose hit points were all in the fiducial volume. This rejected the nuclear-track background events from the fluoroplastic walls of the detection volume.
- Energy selection: We selected events whose energy is between $100\text{ keV}\alpha.\text{e}$.¹ and $400\text{ keV}\alpha.\text{e}$. The lower energy threshold is chosen so as to maintain a certain angular resolution, which is restricted by the length of the nuclear recoil. The higher one is set at the expected highest recoil energy of WIMPs at escape velocity. We refer to this as the DM energy range in the following discussion.
- Nuclear-recoil selection: We select events with track lengths shorter than 1 cm. The length limit rejects background γ -ray events.

We review the methods and results of detector performance measurements in the following paragraphs. Details can be found in ref [32].

¹ $100\text{ keV}\alpha.\text{e}$. corresponds to 140 keV fluorine recoil, for reference.

- Energy resolution: The energy resolution was determined by three components: the electric noise term (σ_{noise}), the gain non-uniformity term ($\sigma_{\text{non-uni}}$), and statistics of the primary ion-electron pair term (σ_{sta}). σ_{noise} was measured to be 55%, $\sigma_{\text{non-uni}}$ was known to be 45% from the high-energy (6 MeV $\alpha.e.$) peaks, and σ_{sta} was calculated to be 6%. Thus, the squared sum of these three terms gives an energy resolution of 70% (FWHM) at 100 keV $\alpha.e.$
- γ -ray detection efficiency: We irradiated the NEWAGE-0.3a with γ -rays from a ^{137}Cs radioactive source. We compared the detection rate of electron tracks that passed event selection with a simulated rate; the detection efficiency was found to be 8.1×10^{-6} at 100 keV $\alpha.e.$ Thus, the γ -ray rejection power was 99.9992% at 100 keV $\alpha.e.$ The energy dependence is shown in our previous work[32].
- Nuclear track absolute detection efficiency: We irradiated the NEWAGE-0.3a with neutrons from a ^{252}Cf radioactive source. We compared the rate of detected nuclear tracks that passed event selection with the simulated rate. The nuclear track detection efficiency was found to be 80% at 100 keV $\alpha.e.$ The energy dependence is shown in our previous work[32]. The measured energy dependence was taken into account in the analysis of dark matter run data.
- Direction-dependent nuclear track detection efficiency: We irradiated the NEWAGE-0.3a with neutrons from a ^{252}Cf radioactive source. We made isotropic scattering by placing the source at six positions and measured the direction-dependent nuclear track detection efficiency.
- Nuclear track angular resolution: We irradiated the NEWAGE-0.3a with neutrons from a ^{252}Cf radioactive source. We fitted the $|\cos \theta|$ distribution of recoil nuclear tracks with simulated ones smeared by various angular resolutions. θ is the angle between the direction of the incident neutron and that of a detected nuclear track. We obtained an angular resolution

Table 1: Performance of NEWAGE-0.3a detector at energy threshold (100 keV α .e.)[32].

Parameter	Value
Energy resolution	70% (FWHM)
γ -ray detection efficiency	8.1×10^{-6}
Nuclear track detection efficiency	80%
Nuclear track angular resolution	55° (RMS)

Table 2: Summary of NEWAGE-0.3a first underground dark matter run (N03aKa-Run5).

Sub-Runs	Date	Live Time [days]	Exposure [kg·days]
Run5-1	Sep. 11th – Oct. 1st, 2008	17.81	0.204
Run5-2	Oct. 2nd – Nov. 11th, 2008	10.01	0.115
Run5-3	Nov. 13th – Dec. 4th, 2008	17.90	0.205
Total exposure			0.524

of 55° (RMS) for 100 keV α .e. nuclear tracks.

Typical results of performance measurement are listed in TABLE 1.

3. Measurements

The first underground dark matter run with the NEWAGE-0.3a detector took place from September 11, 2008 until December 4, 2008 in Laboratory B, Kamioka Observatory ($36^\circ 25'N$, $137^\circ 18'E$) located at 2700 m water-equivalent underground. The detector was set so that the μ -PIC plane was horizontal and the X-axis was aligned in the direction of $S87^\circ E$. Since the fast neutron flux in the underground laboratory was smaller than that in the surface laboratory by more than three orders of magnitude, the background in this first underground run was expected to be dominated by the internal background. Therefore, we did not set any radiation shield. This dark matter run (N03aKa-Run5) has three sub-runs, as listed in TABLE 2. We evacuated and refilled the vessel with new CF_4 gas at the beginning of each sub-run.

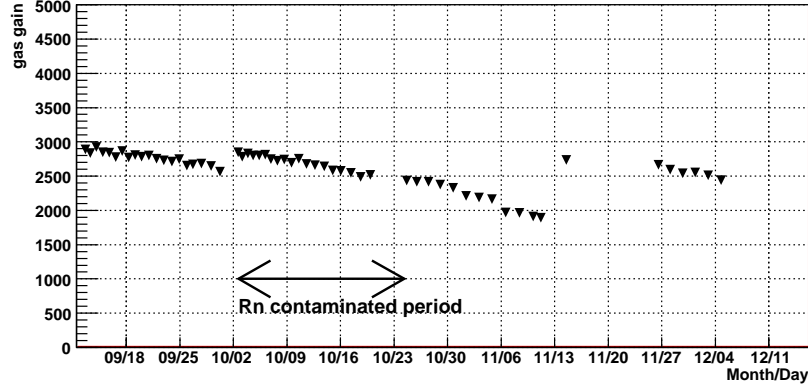


Figure 2: Monitored gas gain during Run5.

We monitored the gas gain and the radioactive radon (^{220}Rn and ^{222}Rn) contamination in the gas using high-energy ($\sim 6 \text{ MeV}\alpha.e.$) events. The gas gain was monitored by the positions of the high-energy radon peaks. The monitored gas gains were used to correct the energy calibration. The radioactive radon rate was monitored by the count rate of high-energy peaks so as to monitor part of the internal radioactivity. The monitored gas gain and radioactive radon rate are shown in FIG. 2 and FIG. 3, respectively. We found that we unintentionally contaminated the target gas with radioactive radon gas by using a vacuum tube and turbo molecular pump exposed to mine air during the gas replacement procedure at the beginning of Run5-2. We therefore did not use this period for further analysis (indicated in FIG. 2 and 3). Live times and exposures excluding this radon-contaminated period are shown in the run summary (TABLE 2). A total exposure of 0.524 kg-days was accumulated in about three months' measurement.

4. Results

4.1. Measured Data

We applied the data selection criteria described in Section 2.2 to the entire 0.524 kg-days of Run-5 dark matter data. 1244 nuclear tracks passed through

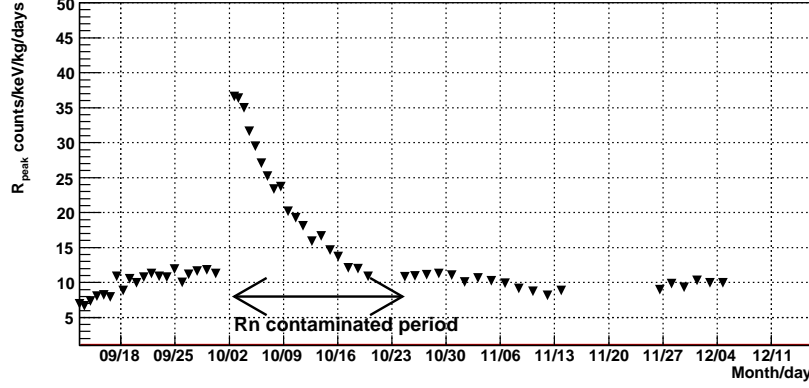


Figure 3: Monitored radon progeny count rate during Run5.

the selections. We corrected the count rate using the detection efficiency and obtained the energy spectrum shown in FIG.4. The count rate at the energy threshold of $100\text{keV}\alpha.e.$ was about $50\text{ counts/keV/kg/days}$. We also plotted the directions of all 1244 nuclear recoil tracks (shown by black markers in FIG.5 (A)). Because we did not detect the sense of the nuclear tracks (track detection was axial-like and not vector-like), the map was restricted to half the sky. The southern part of the sky was folded into the northern half. We then performed a direction-sensitive analysis assuming isotropic WIMP motion, *i.e.*, WIMP-wind from the Cygnus direction. The direction toward Cygnus at each event time was also indicated by purple markers. We calculated θ , the angle between the recoil direction (black markers) and the corresponding WIMP-wind direction (purple markers) for each event, and made a $|\cos\theta|$ distribution which is shown in FIG. 5 (B). The $|\cos\theta|$ distribution is normalized with the energy range, the target mass, and live time, while it still contains detector responses such as the energy resolution, angular resolution, and detection efficiencies.

4.2. Direction-Sensitive Analysis

We derived direction-sensitive dark matter limits by comparing the measured $|\cos\theta|$ distribution with those expected from WIMP-nucleus elastic scatterings.

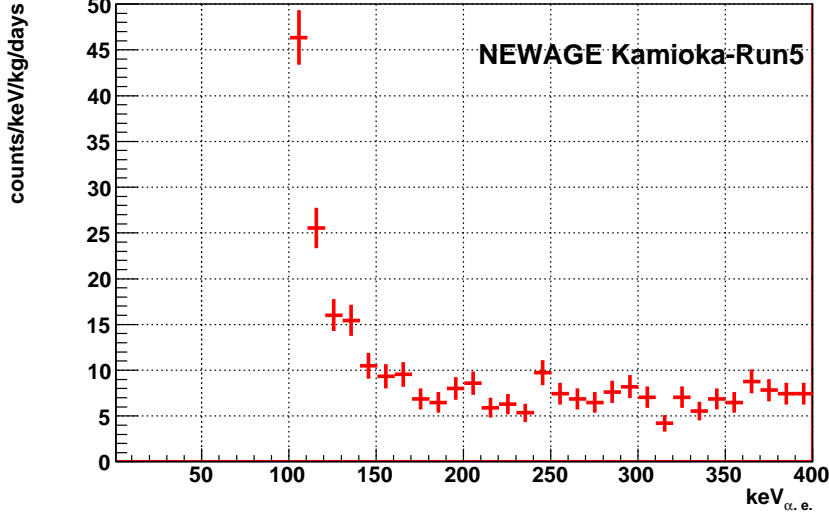


Figure 4: Measured energy spectrum. The total exposure was 0.524 kg-days.

We used the astrophysical and nuclear parameters given in Table 3. We used the same analysis procedure described in our previous work [31] unless otherwise stated. We prepared the expected $|\cos \theta|$ distributions for given WIMPs masses and energy bins. We considered the detector response, such as the energy resolution, angular resolution, and detection efficiencies, to make these expected $|\cos \theta|$ distributions. Followings are the procedure for preparing this expected $|\cos \theta|$ distribution.

We followed ref. [35] for the energy-spectrum calculation. An ideal $|\cos \theta|$ distribution without detector responses can be calculated by equation 1, where R is the count rate, θ is the recoil angle, v_s is the solar velocity with respect to the galaxy, v_{\min} is the minimum velocity of WIMPs that can give a recoil energy of E_R , and v_0 is the Maxwellian WIMP velocity dispersion [36, 22].

$$\frac{d^2 R}{dE_R d\cos \theta} \propto \exp \left[\frac{(v_s \cos \theta - v_{\min})^2}{v_0^2} \right] \quad (1)$$

With the expected energy spectrum and the $|\cos \theta|$ distribution known from equation 1, we made a two-dimensional event rate “spectrum” which is a func-

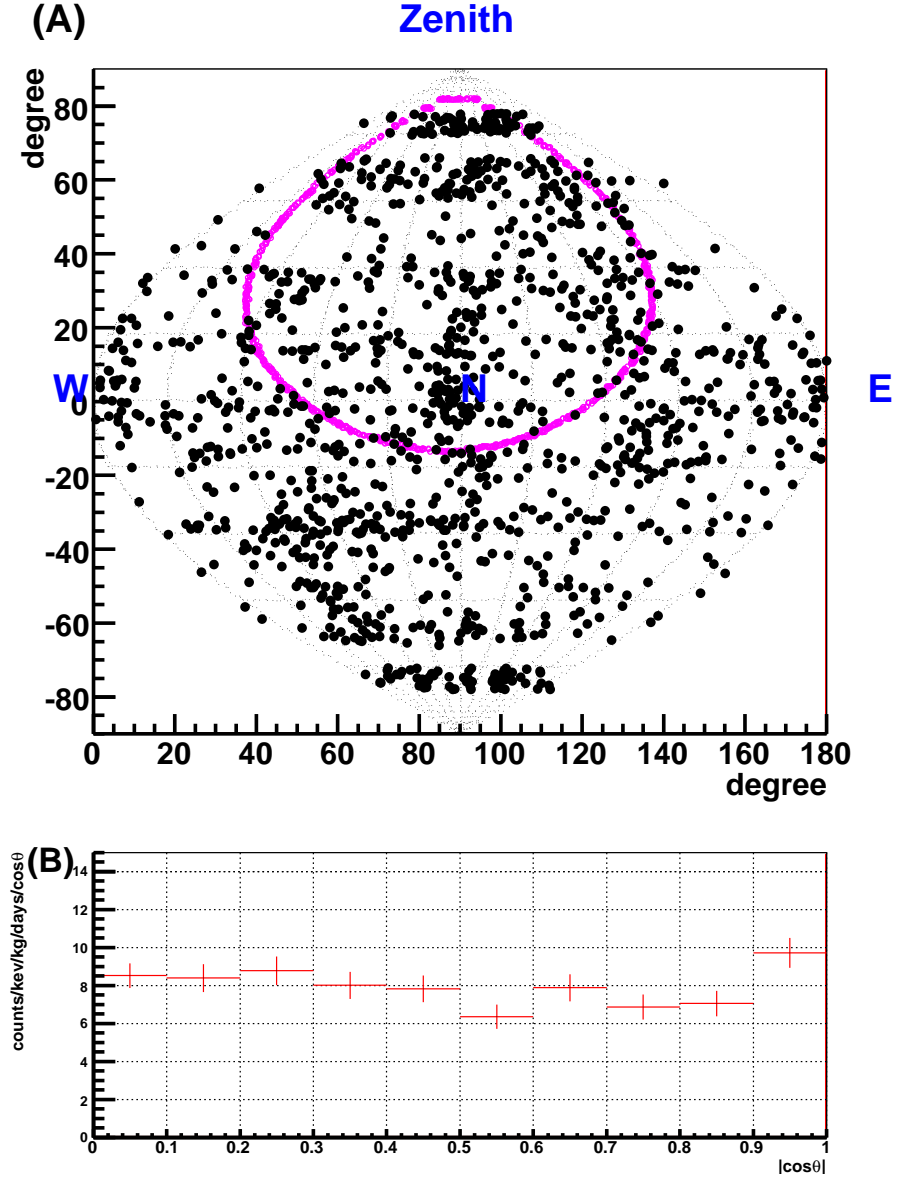


Figure 5: Obtained directions of the nuclear tracks (A) and $|\cos \theta|$ distribution(B). Black markers in (A) indicate directions of the 1244 nuclear track events. The direction toward Cygnus from which the WIMP-wind is expected at each event time is indicated by purple markers in (A).

tion of the recoil angle and recoil energy (shown in FIG. 6).

The horizontal slice of this two-dimensional spectrum is the ideal $|\cos \theta|$ distribution corresponding to the energy range of interest. We took account of the detector response by the following steps.

- STEP 1: (For a given WIMP mass) We made an ideal two-dimensional event rate “spectrum” distribution like that shown in FIG. 6.

The input parameter is a WIMP mass. The output is the two-dimensional event rate “spectrum”.

- STEP 2: (For a given WIMP-wind direction) We simulated a WIMP-nucleus scattering in the actual detector coordinates. The recoil energy and angle θ_R were generated according to the distribution calculated in STEP 1. Here, we convert the recoil energy into alpha-equivalent energy, considering the ionization efficiencies, or quenching factors, of the fluorine and helium nuclei using the SRIM code[37]. The azimuth angle of the recoil, ϕ_R , was randomly determined.

The input parameter is a WIMP-wind direction. The output parameters are the direction and energy of a nuclear track in a detector.

- STEP 3: We calculated the detection efficiency as a product of the absolute detection efficiency which is a function of energy, and the relative efficiency which is a function of the track direction.

Input parameters are the energy and direction of a nuclear track (result of STEP 2). Output parameter is the detection efficiency.

- STEP 4: We calculated the observable energy and direction by smearing the actual energy and direction according to the resolutions.

The input parameters are the actual energy and direction energy of a nuclear track (result of STEP 2). The output parameters are the observable direction and energy.

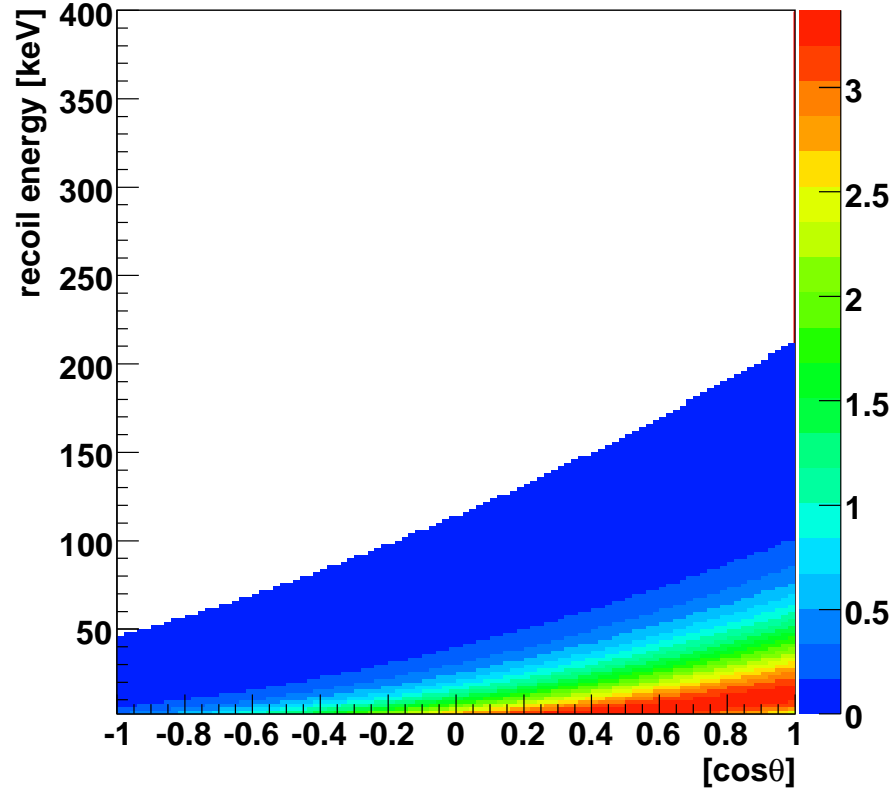


Figure 6: Expected two-dimensional event rate “spectrum” as a function of the recoil angle and recoil energy. The target is fluorine nuclei. A WIMP mass of $100 \text{ GeV}/c^2$ and a cross section of 1 pb are assumed. θ is the recoil angle of the nuclear recoil with respect to the WIMP-wind direction. Color contour shows event rate in the unit of $[\text{counts/keV/kg/days}/\cos\theta]$. White areas are the parameter space where no event is expected.

- STEP 5: We calculated $|\cos\theta|$ using the observable track direction (result of STEP 4) and the WIMP-wind direction (input parameter of STEP 2). We filled the $|\cos\theta|$ histogram of the energy bin of interest with the calculated $|\cos\theta|$. We used the efficiency calculated in STEP 3 as the weight for filling.
- STEP 6: We repeated STEPS 2 to 5 for many WIMP-wind directions to reproduce the actual direction distribution of the WIMP-wind during the observation time.
- STEP 7: We repeated STEPS 1 to 6 for the WIMP masses of interest.

In this way, we made $|\cos\theta|$ distributions expected from WIMP-nucleus elastic scatterings.

4.3. Dark Matter Limits

We finally set the direction-sensitive dark matter limits. Here we conservatively treated all of the 1244 nuclear recoil events as dark matter events without any background subtraction. Because the $|\cos\theta|$ distribution has an energy dependence and the statistics were not very large, we made two-bin $|\cos\theta|$ histograms for 15 energy ranges. We show one of the $|\cos\theta|$ histograms with a best-fitted expected WIMP signal in FIG. 7. The energy range and mass of the WIMP are 100–120 keV α .e. and 100 GeV/ c^2 , respectively. The best-fitted cross section of 5500 pb yielded a χ^2/dof of 3.71/1 and this expected WIMP signal was rejected at a 90% confidence level by a χ^2 test in this case. We then fitted the $|\cos\theta|$ distributions with the expected WIMP signals for the other 14 energy ranges. We took the smallest cross section as a limit for the WIMP mass (in this case, 100 GeV/ c^2). We calculated the limits for WIMPs with masses from 30 GeV/ c^2 to 1000 GeV/ c^2 in the same manner. The WIMP-signal $|\cos\theta|$ distributions expected with all of the WIMP masses were rejected by χ^2 tests.

The obtained upper limits of the SD WIMP-proton cross section are shown in FIG. 8. The best limit was 5400pb for WIMPs with a mass of 150 GeV/ c^2 .

Table 3: Astrophysical and nuclear parameters used to calculate the WIMP-proton cross section limits.

WIMP velocity distribution	Maxwellian
Solar velocity	$v_s = 244\text{kms}^{-1}$
Maxwellian velocity dispersion	$v_0 = 220\text{kms}^{-1}$
Escape velocity	$v_{\text{esc}} = 650\text{kms}^{-1}$
Local halo density	0.3GeVcm^{-3}
Spin factor of ^{19}F	$\lambda^2 J(J+1) = 0.647$

This result marked a new sensitivity record for an SD WIMP search with the direction sensitive method.

We also fitted the measured $|\cos\theta|$ distribution with the isotropic background model. The fitting result gave $\chi^2/\text{d.o.f.} = 0.110/1$ independent of the WIMP mass, and the isotropic background model was not rejected at 90% confidence level.

5. Discussions

5.1. Background

We studied the origin of the background for future improvement of the sensitivity. We discuss the estimated contribution of various background sources to the count rate at the energy threshold of 100 keV α .e. Details will be reported elsewhere.

We started the study with the background from outside the vessel. The measured flux of fast neutrons was $1.9 \times 10^{-6} \text{cm}^{-2} \text{s}^{-1}$ [40], and their contribution at 100 keV α .e. was simulated to be less than 0.2 counts/keV/kg/days. We measured the γ -ray flux in our laboratory and simulated the contribution of γ -rays, considering the γ -ray detection efficiency. The contribution of γ -rays was simulated to be less than 7_{-4}^{+7} counts/keV/kg/days. The cosmic-ray muon flux at Kamioka Observatory is $6 \times 10^{-8} \text{cm}^{-2} \text{s}^{-1} \text{sr}^{-1}$ [41]. The muon rate passing through the effective volume of the μ -TPC was calculated to be less than

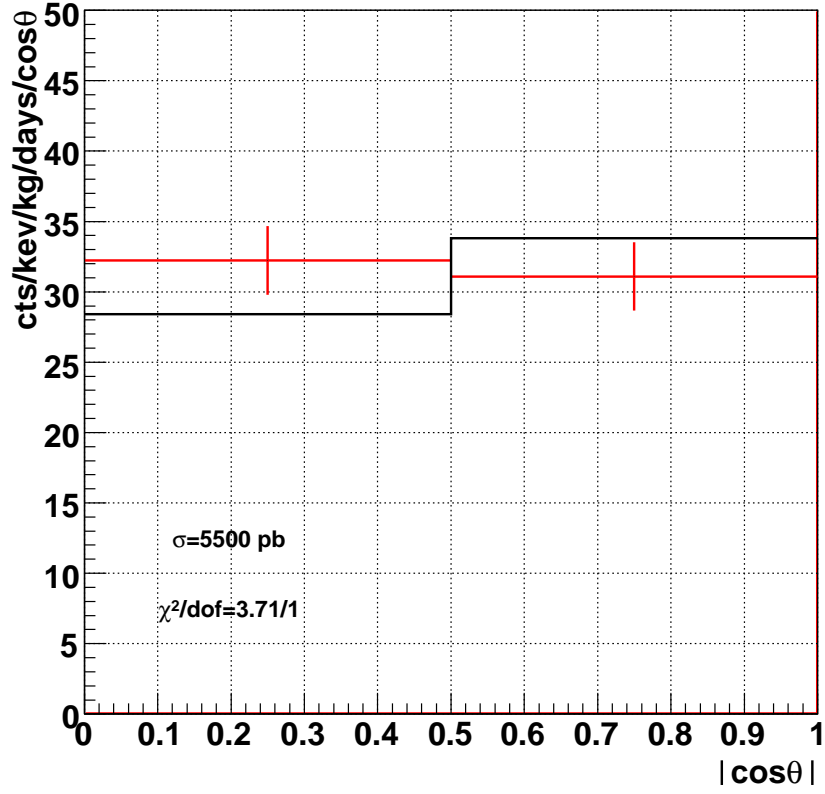


Figure 7: Measured $|\cos \theta|$ distributions of Kamioka Run-5 (histogram with error bars, red online) and the best-fitted expected $|\cos \theta|$ distribution (histogram without error-bars, black online). The energy range and mass of the WIMP are 100–120 keV α .e. and 100 GeV/ c^2 , respectively. The best-fitted cross section of 5500 pb yielded $\chi^2/\text{dof} = 3.71/1$, and this expected WIMP signal was rejected at a 90% confidence level by a χ^2 test.

SD 90% C.L. upper limits and allowed region

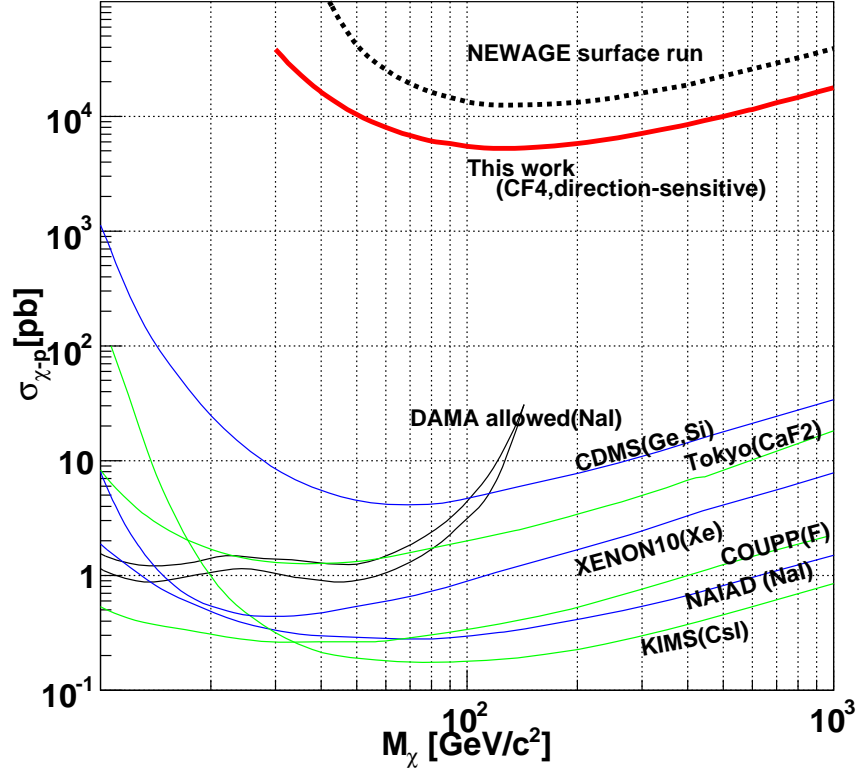


Figure 8: Upper limits and allowed region in the WIMP-proton spin-dependent cross section versus WIMP mass parameter space. Thick solid line shows the limits obtained in this work. Limits from our surface run[31] are shown by a thick-dotted line for comparison. Limits and allowed region from other direction-insensitive WIMP-search experiments (DAMA(NaI)[9], CDMS[38], Tokyo CaF₂[12], XENON10[39], COUPP[16], NAIAD[11], KIMS[15]) are shown for reference.

2×10^{-4} counts/s. We assumed the rejection power of electrons, 8×10^{-6} , as an upper limit to that of muons. Then the rate of muon tracks misidentified as nuclear tracks should be less than 0.2 counts/kg/days above 100 keV α .e. The secondary particles produced by cosmic-ray muons are studied as ambient gamma rays and neutrons in previous discussions.

Next, we studied background sources within the vessel. Radioactive isotopes in the ^{238}U and ^{232}Th chains are the main background sources in many rare-event measurements. We first studied the contribution of the radon gas (^{220}Rn , ^{222}Rn , and their progeny) by a radon-rich run. (We intentionally contaminated the detector with radon gas in the same way as we unintentionally did at the beginning of Run5-2.) We found that the radon gas accounted for about 5 counts/keV/kg/days at 100keV α .e. We then studied the contribution of alpha particles emitted from materials exposed to the detection volume. It is known that alpha particles from the surface of the materials would deposit part of the entire energy in the detection volume and would make background events in the DM energy range. We simulated the energy depositions of these surface- α events and found that the upper limits of their contribution can be known by the measured count rate around 1 MeV α .e. We thus found that these surface- α events, other than the partial energy deposition in the thin (5 mm) volume between the μ -PIC and the GEM (gap events, see FIG. 1), made negligible contributions. The gap events were found to potentially explain the remaining background. We found that the relative gas gains of the GEM and μ -PIC affect the contributions of gap events to the count rate around 100keV α .e; namely, a higher GEM-gain yields a lower count rate and vice versa. Because higher GEM-gain operation would increase the risk of fatal damage to the GEM, we performed a lower GEM-gain run to test this possibility. The count rate actually increased in the lower GEM-gain run.

We summarize the results of the background study in Table 4. The results indicate we can potentially explain the background with the the gap events and ambient gamma-ray events. We are making efforts to reduce these two main sources of the background to improve the sensitivity.

Table 4: Results of background studies. The rates at the energy threshold are shown in the unit of [counts/kg/days/keV] .

source	rate
Ambient gammas	~ 10
Ambient fast neutrons	$\sim 10^{-1}$
Cosmic muons	$< 2 \times 10^{-1}$
Internal α (fiducial volume)	$< 10^{-1}$
Internal α (gap volume)	< 40
Internal β	< 5
Measured(Run5)	50

6. Conclusions

A direction-sensitive dark matter search experiment in the Kamioka underground laboratory with the NEWAGE-0.3a detector was performed. The measurements were performed from September 11, 2008 until December 4, 2008, producing a total exposure of 0.524 kg·days. As a result of this experiment, improved spin-dependent WIMP-proton cross section limits by a direction-sensitive method, including a new record of 5400 pb for 150 GeV/c² WIMPs, were achieved.

Acknowledgments

This work was partially supported by Grant-in-Aids for KAKENHI (19684005) of Young Scientist(A); JSPS Fellows; and Global COE Program “The Next Generation of Physics, Spun from Universality and Emergence” from the Ministry of Education, Culture, Sports, Science and Technology (MEXT) of Japan.

References

- [1] J. Dunkley et al. (SDSS), *AstroPhys. J.* 701 (2009) 1804.
- [2] M. Tegmark et al. (SDSS), *Astrophys. J.* 606 (2004) 702.

- [3] M. Tegmark et al. (SDSS), Phys. Rev. D 69 (2004) 103501.
- [4] A. G. Riess et al., Astron. J. 116 (1998) 1009.
- [5] S. Perlmutter et al., Astrophys. J. 517 (1999) 565.
- [6] J. Ellis et al., Phys. Lett. B 603 (2004) 51.
- [7] A. A. Abdo et al., Phys Rev. Lett. 102 (2009) 181101.
- [8] F. Aharonian et. al (HESS collaboration), Phys. Rev. Lett. 97 (2006) 221102.
- [9] R. Bernabei et al., Phys. Lett. B 480 (2000) 23.
- [10] J. Angle, et al. (XENON Collaboration), Phys. Rev. Lett. 100 (2008) 021303.
- [11] B. Ahmed et al., Astropart. Phys. 19 (2003) 691.
- [12] Y. Shimizu et al., Phys. Lett. B 633 (2006) 195.
- [13] D.S. Akerib et al. (CDMS Collaboration), Phys. Rev. D 72 (2005) 052009.
- [14] R. Bernabei et al., Eur. Phys. J. C 56 (2008) 333.
- [15] H. S. Lee, et al. (KIMS Collaboration), Phys. Rev. Lett. 99 (2007) 091301.
- [16] E. Behnke et al., Science 319 (2008) 933.
- [17] H. P. Nilles, Phys. Rep. 110 (1984) 1.
- [18] A. M. Green and B. Morgan, Astropart. Phys. 27 (2007) 142.
- [19] P. Belli et.al, Nuovo Cimento C 15 (1992) 473.
- [20] R. Bernabei et.al, Eur. Phys. C 28 (2003) 203.
- [21] H. Sekiya et.al, Proceedings of Fifth International Workshop on the Identification of Dark Matter (2004) 378.
- [22] K. N. Buckland et al., Phys. Rev. Lett. 73 (1994) 1067.

- [23] T. Tanimori et al., Phys. Lett. B 578 (2004) 241.
- [24] D. Dujmic et al., Astropart. Phys. 30 (2008) 58.
- [25] T. Naka et al., Nucl. Instrm. Methods Phys. Res. Sect. A 581 (2007) 761.
- [26] J. Rich, M. Spiro, Saclay preprint DPhPE 88-04.
- [27] G. Masek et al., Proceedings of the Workshop on Particle Astrophysics (1989) 43.
- [28] G. Gerbier et al., Proceedings of the Workshop on Particle Astrophysics (1989) 43.
- [29] H. Burgos et al., Nucl. Instrm. Methods Phys. Res. Sect. A 600 (2009) 417.
- [30] H. Burgos et al., Astropart. Phys. 28 (2007) 409.
- [31] K. Miuchi et al., Phys. Lett. B 654 (2007) 58.
- [32] H. Nishimura et al., Astropart. Phys. 31 (2009) 185.
- [33] A. Takada et al., Nucl. Instrm. Methods Phys. Res. Sect. A 573 (2007) 195.
- [34] F. Sauli, A. Sharma, Annu. Rev. Nucl. Part. Sci 49 (1999) 341.
- [35] J. D. Lewin and P. F. Smith, Astropart. Phys. 6 (1996) 87.
- [36] D. Spergel, Phys. Rev. D 37 (1988) 1353.
- [37] J.F. Ziegler, J.P. Biersack, SRIM The Stopping and Range of Ions in Matter, Code.
- [38] D. S. Akerib, et al. (CDMS Collaboration), Phys. Rev. D 73 (2006) 011102(R).
- [39] J. Angle, et al. (XENON Collaboration), Phys. Rev. Lett. 101 (2008) 091301.
- [40] Private communication with A. Minamino, University of Tokyo,.
- [41] SK Collaboration, Nucl. Instrm. Methods Phys. Res. Sect. A 501 (2003) 418.